

## Interconversion between a Nonporous Nanocluster and a Microporous Coordination Polymer Showing Selective Gas Adsorption

Yan-Juan Zhang, Tao Liu, Shinji Kanegawa, and Osamu Sato\*

*Institute for Materials Chemistry and Engineering, Kyushu University, 6-1 Ksuga-koen, Fukuoka, 816-8580, Japan*

Received October 12, 2009; E-mail: sato@cm.kyushu-u.ac.jp

The preparation of porous metal–organic frameworks (MOFs) with nanosized cavities and/or nanosized open channels has recently received significant attention due to their potential applications in catalysis, gas storage, and separation.<sup>1</sup> One of the current challenges is the design and synthesis of porous MOFs with dynamic changes in structures and functions. Researchers have reported several interesting switchable properties induced by the uptake of guest molecules, among these nanoporous MOFs.<sup>2</sup> One of the most remarkable structural changes in such nanosystems would be the modification of dimensionality between a nonporous nanocluster and a nanoporous MOF in the single crystal state. However, this goal is still a challenge for those transformations involving the breaking/forming of coordination bonds,<sup>3</sup> especially those arising from cooperative solid state reactions and leading to reversibility.<sup>4</sup> Here, we report a reversible conversion from a hexanuclear cluster to a one-dimensional (1D) double-zigzag chain via polymerization and depolymerization in the single crystal state. The framework of the former was nonporous, whereas that of the latter was microporous and displayed selective gas adsorption. Furthermore, accompanying the structural transformation, its functions, i.e. the magnetic properties, also reversibly switched between paramagnetism in the nanocluster and metamagnetism in the 1D chain.

The starting material of the solid state reaction involving switchable porosity and dimensionality is a hexanuclear cluster  $[\{\text{Fe}^{\text{III}}(\text{Tp})(\text{CN})_3\}_4\{\text{Co}^{\text{II}}(\text{CH}_3\text{CN})(\text{H}_2\text{O})_2\}_2] \cdot 10\text{H}_2\text{O} \cdot 2\text{CH}_3\text{CN}$  (Tp = hydrotris(pyrazolyl)borate) (**1**) (Figure 1a), which has been reported by Kim et al.<sup>5</sup> In the neutral hexanuclear unit, two bidentate  $[\text{Fe}(\text{Tp})(\text{CN})_3]^-$  anions linked two  $\text{Co}^{\text{II}}$  ions through cyano bridges, forming an  $[\text{Fe}^{\text{III}}_2\text{Co}^{\text{II}}_2(\text{CN})_4]^{6+}$  square unit. The other two  $[\text{Fe}(\text{Tp})(\text{CN})_3]^-$  anions were monodentate and bonded to two  $\text{Co}^{\text{II}}$  ions. Each  $\text{Co}^{\text{II}}$  further coordinated with one  $\text{CH}_3\text{CN}$  and two  $\text{H}_2\text{O}$  molecules. Ten unbound  $\text{H}_2\text{O}$  and two  $\text{CH}_3\text{CN}$  molecules existed between the cyano-bridged  $\text{Fe}^{\text{III}}_4\text{Co}^{\text{II}}_2$  clusters, mutually linked through hydrogen bonds, generating a 1D neutral molecular tape along the *a* axis (Figure 1a).

Two characteristics of this structure were noteworthy. First, many free solvent molecules were located among the hexanuclear clusters, so a porous framework should have resulted from the removal of the solvent molecules on heating. Second, there was a terminal  $\text{CN}^-$  on the  $[\text{Fe}(\text{Tp})(\text{CN})_3]^-$  moiety and weakly coordinated solvent molecules on the  $\text{Co}^{\text{II}}$  on the two diagonal sides of the square core of  $\text{Fe}^{\text{III}}_2\text{Co}^{\text{II}}_2$ . Hence, once the coordinated solvent molecules were removed on heating, concomitantly, the  $\text{CN}^-$  anions coordinated to the free sites of  $\text{Co}^{\text{II}}$ , allowing a solid state reaction that formed a coordination polymer structure. We performed a thermogravimetric analysis (TGA) measurement to verify the solid state reaction. The TGA curve of **1** displayed a weight loss of 21.8% from 30 to 90 °C, corresponding to the loss of fourteen  $\text{H}_2\text{O}$  molecules and four  $\text{CH}_3\text{CN}$  molecules (21.6%) (Figure S1). Consequent to this weight loss, we observed a long plateau up to 250 °C, suggesting the formation of a new stable phase as shown by the IR spectrum (Figure S2) and powder XRD patterns (Figure

S3). To shed light on the structural changes, we attempted to analyze the crystal structure of the desolvated sample of  $[\text{Fe}^{\text{III}}(\text{Tp})(\text{CN})_3]_2\text{Co}^{\text{II}}$  (**2**) and succeeded in obtaining single crystals suitable for the XRD measurement by slowly heating single crystals of **1** at 150 °C under an  $\text{N}_2$  atmosphere.

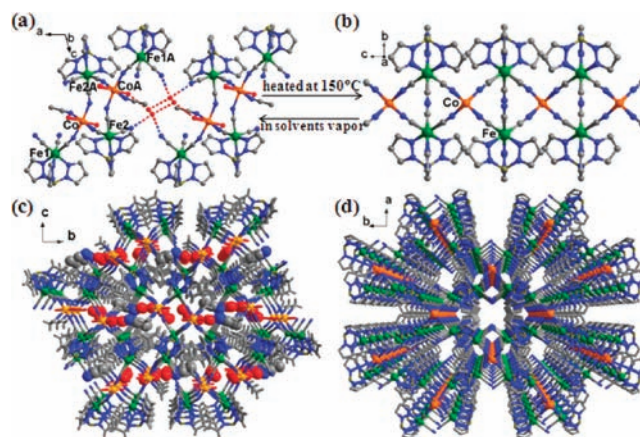


**Figure 1.** (a) Side view of the chain formed by hexanuclear units and a  $(\text{H}_2\text{O})_4$  ring through the hydrogen bonds in **1**. Symmetry operator: A:  $1-x, -y, -z$ . (b) Side view of the 1D double-zigzag chain in **2**. (c) Packing structure of **1**. (d) Packing structure of **2**. Fe, green; Co, orange; N, blue; C, gray; O, red; B, dark yellow. Hydrogen atoms are omitted for clarity.

The single crystal XRD revealed that **2** crystallized in the *Ibam* space. As shown in Figure 1, during the transformation process from **1** to **2**, all uncoordinated and coordinated solvent molecules were lost. Simultaneously, the hexanuclear units moved relative to each other and one of the terminal  $\text{CN}^-$  anions of monodentate  $[\text{Fe}(\text{Tp})(\text{CN})_3]^-$  coordinated to the nearest  $\text{Co}^{\text{II}}$  in the neighboring hexanuclear unit. The distance between the  $\text{Fe}^{\text{III}}$  in  $[\text{Fe}(\text{Tp})(\text{CN})_3]^-$  and the nearest  $\text{Co}^{\text{II}}$  in the neighboring hexanuclear unit was 11.634 Å, while it was 5.051 Å after the formation of the coordination bonds. In this way, the hexanuclear units in **1** became linked, forming the neutral double-zigzag chain of **2** (Figure 1b). Within the neutral double-zigzag chain, each  $[\text{Fe}(\text{Tp})(\text{CN})_3]^-$  entity acted as a bidentate ligand toward two  $\text{Co}^{\text{II}}$  ions through two of its three cyanide groups in the *cis* positions, and each  $\text{Co}^{\text{II}}$  tetrahedrally coordinated to four nitrogen atoms via  $\text{CN}^-$  bridges, affording bimetallic double chains of squares that ran parallel to the *c* axis. The square units showed two orientations of their mean planes ( $\text{Fe}^{\text{III}}_2\text{Co}^{\text{II}}_2$ ) with a dihedral angle of 83.0°. The shortest interchain  $\text{Fe} \cdots \text{Co}$ ,  $\text{Fe} \cdots \text{Fe}$ , and  $\text{Co} \cdots \text{Co}$  distances were 8.576, 7.811, and 11.709 Å, respectively (Table S1). Each chain was further connected with four neighboring chains through the interlocked pyrazolyl rings of the  $[\text{Fe}(\text{Tp})(\text{CN})_3]^-$  units, forming one-dimensional hexagonal channels along the *c* direction in **2** (Figures 1d, S4, and S5). Four interlocked columns of chains surrounded each channel, and the channel walls were composed of the C–H groups of the pyrazolyl rings and the N atoms of the terminal  $\text{CN}^-$  anions. The channel size

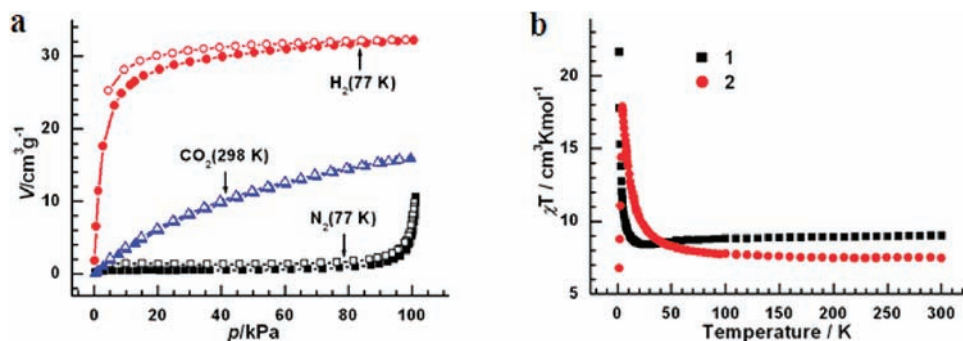


**Figure 2.** (a) Adsorption isotherms of H<sub>2</sub>, N<sub>2</sub>, and CO<sub>2</sub> for **2**. Filled and open symbols represent adsorption and desorption data. (b)  $\chi T$  vs  $T$  plots under a 1 kOe field for **1** and **2**.

was  $1.9 \text{ \AA} \times 3.6 \text{ \AA}$ , excluding the van der Waal radii of the surface atoms, and the void space, calculated using PLATON, was 19.7%. This made **2** different from the chains of  $[\text{Fe}(\text{Tp})(\text{CN})_3]^-$  with  $\text{M}^{\text{II}}$  ( $\text{M} = \text{Mn}, \text{Co}, \text{Ni}$ ) ions, which were synthesized using the general solution mixing method,<sup>6</sup> as all of those structures have no porous frameworks. It clearly showed that conversion from a nonporous cluster to an MOF with nanosized open channels was successfully induced by a solid state reaction.

After exposing compound **2** in a vapor of mixed H<sub>2</sub>O and CH<sub>3</sub>CN, the transformation from **2** to **1** occurred as evidenced by the IR spectrum and powder XRD patterns (Figures S2 and S3), indicating that the transformation was fully reversible. As described previously, the structure after desolvation was an unusual one with tetrahedrally coordinated Co<sup>II</sup>. Hence, to release the strain energy, the reverse process from **2** to **1** was easily induced by just exposing **2** to solvent vapor. It is worth mentioning that chains with the structure of **2** have never been obtained by reactions in solutions. These results confirmed that solid state reactions can provide access to molecules otherwise difficult or impossible to obtain from reactions in solution.

The TGA measurement (Figure S1) showed that **2** was thermally stable until  $\sim 250 \text{ }^\circ\text{C}$ . This stability provided an opportunity for probing gas adsorption properties of the microporous coordination polymer **2**. We investigated the gas adsorption properties of **2** toward small molecules, i.e. N<sub>2</sub>, H<sub>2</sub>, and CO<sub>2</sub>. As shown in Figure 2a, **2** adsorbed CO<sub>2</sub> and H<sub>2</sub> into its pores and showed almost no N<sub>2</sub> uptake, indicating a general correlation between the pore size and kinetic diameters of the adsorbates.<sup>7</sup> Apparently, N<sub>2</sub> could not be adsorbed because its kinetic diameter (3.64–3.80 Å) was larger than the effective channel size. Because of the relatively smaller kinetic diameters of H<sub>2</sub> (2.827–2.89 Å) and CO<sub>2</sub> (3.3 Å), we observed a significant uptake for these gases at 77 and 298 K, respectively. In addition to the size effect, the uptake of CO<sub>2</sub> ( $15.9 \text{ cm}^3 \text{ g}^{-1}$ ) might result from the strong quadrupolar interactions of CO<sub>2</sub> with N atoms present on the pore surface.<sup>7</sup> Moreover, calculations based on the Dubinin–Astakhov (DA) methods gave a pore volume of  $0.050 \text{ cm}^3 \text{ g}^{-1}$  and the isosteric heat of adsorption of CO<sub>2</sub> at 298 K ( $12.5 \text{ kJ mol}^{-1}$ ). The heat of adsorption was far less than those of typical chemical adsorption. Thus, the **2**–CO<sub>2</sub> interaction was mainly physisorptive in nature without significant chemical association. The surface area, determined by fitting the CO<sub>2</sub> adsorption isotherm of **2** to the BET equation, was  $154 \text{ m}^2 \text{ g}^{-1}$ . We observed a steep rise in the adsorption branch of H<sub>2</sub> at extremely low pressures relative to the saturation vapor pressure of H<sub>2</sub>; this high initial uptake indicated the presence of intrinsic micropores in **2**.<sup>7b</sup>

Accompanying the structural conversion, great changes occurred in the magnetic behaviors. As reported by Kim et al.,<sup>5</sup> the interaction between Fe<sup>III</sup> and Co<sup>II</sup> in **1** was antiferromagnetic, with a negative Weiss temperature ( $\Theta = -3.0$ ) given by fitting  $\chi^{-1}$  data to the Curie–Weiss law at temperatures above 30 K. For **2**, however, on cooling, the  $\chi T$  values increased more and more quickly, reaching a very sharp maximum of  $17.8 \text{ cm}^3 \text{ K mol}^{-1}$  at 4.4 K (Figure 2b),

fitting  $\chi^{-1}$  data to the Curie–Weiss law above 30 K and providing a positive Weiss temperature ( $\Theta = 5.6$ ). It indicated the ferromagnetic interactions between Fe<sup>III</sup> and Co<sup>II</sup> in **2**. Moreover, the  $\chi T$  value at room temperature changed from  $9.0 \text{ cm}^3 \text{ K mol}^{-1}$  for **1** to  $7.4 \text{ cm}^3 \text{ K mol}^{-1}$  for **2** due to the different contributions of the orbital angular momentum of Co<sup>II</sup> with octahedral and tetrahedral coordination geometries, verifying the hypothesis of Kim et al.<sup>5</sup> Further magnetic investigation revealed that **1** was a paramagnet, whereas **2** was a metamagnet due to the weak interchain antiferromagnetic interactions with a critical field of 4.5 kOe and Neel temperature of 4.0 K (Figures S6–S10).

In summary, we succeeded in obtaining the interconversion of a paramagnetic nonporous hexanuclear cluster to a metamagnetic porous double-zigzag chain through reversible polymerization and depolymerization in a single crystal state and in which the porous state displayed selective gas adsorption. The conversion accompanied a change in their magnetic properties. The reversible polymerization and depolymerization reaction in a single crystal state provided a novel method for preparing multifunctional nanoporous MOFs with switchable structures and functions.

**Acknowledgment.** This work was supported by a Grant-in-Aid for Scientific Research (A) from the Ministry of Education, Culture, Sports, Science and Technology, Japan. We thank the BEL Japan company for the gas adsorption measurement.

**Supporting Information Available:** X-ray crystallographic file in CIF format for **2**, a PDF file containing further information about the experiments, Table 1, and Figures S1–S10. This material is available free of charge via the Internet at <http://pubs.acs.org>.

## References

- (a) Ma, L.; Abney, C.; Lin, W. *Chem. Soc. Rev.* **2009**, *38*, 1248. (b) Das, M. C.; Bharadwaj, P. K. *J. Am. Chem. Soc.* **2009**, *131*, 10942. (c) Wang, B.; Côté, A. P.; Furukawa, H.; O’Keeffe, M.; Yaghi, O. M. *Nature* **2008**, *453*, 207. (d) Pan, L.; Olson, D. H.; Ciemmolonski, L. R.; Heddy, R.; Li, J. *Angew. Chem., Int. Ed.* **2006**, *45*, 616. (e) Serre, C.; Mellot-Drazniewski, C.; Surblé, S.; Audebrand, N.; Filinchuk, Y.; Férey, G. *Science* **2007**, *315*, 1828.
- (a) Kurmoo, M.; Kumagai, H.; Chapman, K. W.; Kepert, C. J. *Chem. Commun.* **2005**, 3012. (b) Ohba, M.; Yoneda, K.; Agustí, G.; Muñoz, M. C.; Gaspar, A. B.; Real, J. A.; Yamasaki, M.; Ando, H.; Nakao, Y.; Sakaki, S.; Kitagawa, S. *Angew. Chem., Int. Ed.* **2009**, *48*, 4767.
- (a) Vittal, J. J. *Coord. Chem. Rev.* **2007**, *251*, 1781. (b) Cheng, X.-N.; Zhang, W.-X.; Chen, X.-M. *J. Am. Chem. Soc.* **2007**, *129*, 15738.
- (a) Campo, J.; Falvello, L. R.; Mayoral, I.; Palacio, F.; Soler, T.; Tomás, M. *J. Am. Chem. Soc.* **2008**, *130*, 2932–2933. (b) Kaneko, W.; Ohba, M.; Kitagawa, S. *J. Am. Chem. Soc.* **2007**, *129*, 13706. (c) Duan, Z.; Zhang, Y.; Zhang, B.; Zhu, D. *J. Am. Chem. Soc.* **2009**, *131*, 6934.
- Kim, J.; Han, S.; Pokhodnya, K. I.; Migliori, J. M.; Miller, J. S. *Inorg. Chem.* **2005**, *44*, 6983.
- (a) Wen, H.-R.; Wang, C.-F.; Song, Y.; Gao, S.; Zuo, J.-L.; You, X.-Z. *Inorg. Chem.* **2006**, *45*, 8942. (b) Jiang, L.; Feng, X.-L.; Lu, T.-B.; Gao, S. *Inorg. Chem.* **2006**, *45*, 5018.
- (a) Li, J.-R.; Kuppler, R. J.; Zhou, H.-C. *Chem. Soc. Rev.* **2009**, *38*, 1477. (b) Zou, Y.; Hong, S.; Park, M.; Chun, H.; Lah, M. S. *Chem. Commun.* **2007**, 5182.

JA908670U